The MPI CyberMotion Simulator: A Novel Research Platform to Investigate Human Control Behavior

Frank M. Nieuwenhuizen

Max Planck Institute for Biological Cybernetics, Tübingen, Germany
frank.nieuwenhuizen@tuebingen.mpg.de

Heinrich H. Bülthoff[*]

Max Planck Institute for Biological Cybernetics, Tübingen, Germany
Department of Brain and Cognitive Engineering, Korea University, Seoul, Korea
heinrich.buelthoff@tuebingen.mpg.de

Abstract
The MPI CyberMotion Simulator provides a unique motion platform, as it features an anthropomorphic robot with a large workspace, combined with an actuated cabin and a linear track for lateral movement. This paper introduces the simulator as a tool for studying human perception, and compares its characteristics to conventional Stewart platforms. Furthermore, an experimental evaluation is presented in which multimodal human control behavior is studied by identifying the visual and vestibular responses of participants in a roll-lateral helicopter hover task. The results show that the simulator motion allows participants to increase tracking performance by changing their control strategy, shifting from reliance on visual error perception to reliance on simulator motion cues. The MPI CyberMotion Simulator has proven to be a state-of-the-art motion simulator for psychophysical research to study humans with various experimental paradigms, ranging from passive perception experiments to active control tasks, such as driving a car or flying a helicopter.

I. INTRODUCTION

Motion simulators are increasingly used for training purposes, and provide an effective, efficient, and safe environment for practicing maneuvers outside a real vehicle. The characteristics of the vehicles that these simulators represent are simulated to various degrees. For example, the complete cockpit of a commercial aircraft is used in full flight simulators, whereas a generic representation of a typical car is employed in driving schools.

The motion system of training simulators varies depending on the application scenario. Driving simulator schools require a cost-effective solution, and typically provide onset cues and vibrational cues through a motion seat, if motion is provided at all. In contrast, full flight simulators are typically equipped with hexapod motion platforms to reproduce the motion experienced in flight as faithfully as possible, and to provide the pilot with a realistic training environment [1].

All motion simulators have a limited motion range and

are never able to completely simulate all of the motion cues experienced in a real vehicle [1, 2]. Therefore, motion cueing filters that scale down motion cues considerably and introduce phase shifts are required. In addition, these filters introduce false cues as the simulator needs to be returned to its neutral position. Therefore, the motion experienced by the operator does not reflect the actual state of the vehicle. Despite these limitations, simulator motion is still used in flight training, as it is expected that if a pilot would train without simulator motion, the presence of motion cues in real flight could be disorienting and have a detrimental effect on performance [1]. Similarly, trainees could adapt their behavior, which would result in incorrect control behavior in a real aircraft [3]

The effectiveness of simulator motion has been the subject of many studies on subjects such as the assessment of training and pilot control behavior in closed-loop control tasks. However, the results from these studies provide inconclusive evidence on the effectiveness of simulator motion. In general, the advantages of simulator motion have not been confirmed in transfer-of-training studies for the type of motion offered by Level D full flight simulators [4, 5]. Pilots take advantage of motion cues without needing specific training, and the differences in pilot performance and behavior are generally not operationally relevant [6]. On average, simulator motion seems to have a positive effect when combining results from various transfer-of-training studies in a single analysis [7]. This is due to the importance of whole-body motion when flight-naive participants need to learn highly dynamic flight tasks, whereas motion might not be needed for experts refreshing their maneuvering skills.

In other types of experiments, a positive influence of the availability of simulator motion is found in target-following and disturbance-rejection during closed-loop control tasks [8-11]. In these experiments, simulator motion provides complementary cues to visual cues. Providing participants with simulator motion significantly changes pilot control behavior.

At the Max Planck Institute (MPI) for Biological Cybernetics in Tübingen, Germany, the influence of motion cues on pilot perception and behavior is investigated by performing low-level perception experiments and closed-loop control tasks with humans in the loop. Such experimental paradigms can be used to understand and model perception and behavior in the context of driving a car or flying a helicopter. This introduces the MPI CyberMotion Simulator, a state-of-the-art motion platform for performing such experiments. Its capabilities are contrasted with those of conventional Stewart platform simulators, and experimental results in a helicopter hover task are presented.

II. CONVENTIONAL SIMULATORS

Simulators are predominantly used for training purposes, although they are also deployed for engineering tasks and research. The majority of simulators that provide motion capabilities with 6 degrees of freedom are based on a parallel (or hexapod) design [12]. Such systems are called Stewart platforms, and are equipped with 6 linear actuators that are capable of carrying large payloads and maintaining high rigidity [13].

An MPI example of a Stewart platform is given in Fig. 1. The characteristics of the simulator are summarized in Table 1. The simulator features electric actuators, like many modern full flight simulators. The actuator stroke is
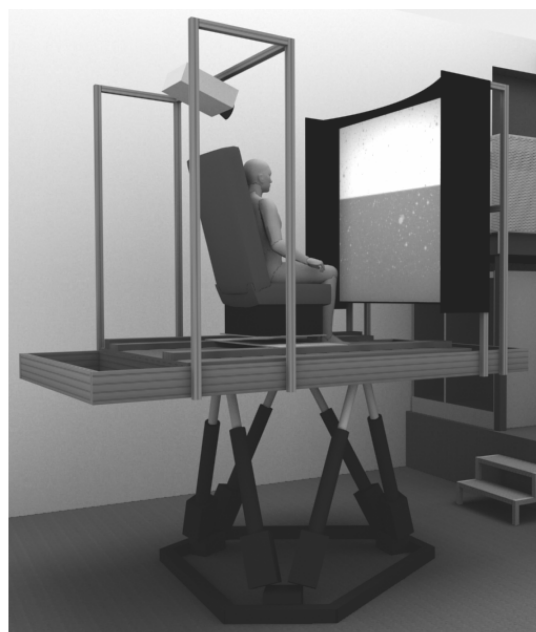
Fig. 1. The MPI Stewart platform.

Table 1. Characteristics of the MPI Stewart platform

Actuators	
Stroke (m)	0.45
Max. velocity (m/s)	0.3
Max. acceleration (m/s^2)	2
Range	
Surge (mm)	922
Sway (mm)	848
Heave (mm)	500
Roll (deg)	±26.6
Pitch (deg)	+24.1/-25.1
Yaw (deg)	±43.5
Time delay (ms)	35

limited compared to larger motion platforms, which results in a limited translational range. The rotational degrees of freedom are similar to many Stewart platforms, as they depend more on the actuator layout than on their stroke.

Generally, the fidelity of a simulator is quantified by assessing the degree to which it reproduces the exact state of the simulated vehicle, and technology-centered metrics are used as classification criteria. For example, motion system hardware is characterized by mechanical properties such as bandwidth and time delay. These characteristics can be measured and reported with a systematic approach [14], although simulator manufacturers are reluctant to publish specifications on their motion system characteristics.

Similarly, surprisingly few criteria have been developed to summarize the findings of extensive research on the requirements for motion provided by Stewart platforms [15]. The Sinacori criterion is most widely used. This criterion aims to provide fidelity boundaries for the motion cueing filters that filter the output of the vehicle dynamics model such that the simulator remains within its limits. The criterion shows that the fidelity of the motion cues decreases when the filter gain decreases or the phase shift introduced by the filters increases.

Although a Stewart platform is very suitable for training applications, its parallel motion system can limit the application of the simulator for research into human perception and behavior. A Stewart platform cannot attain unusual attitudes, as its workspace is limited to a volume around the neutral point of the simulator. Therefore, the Max Planck Institute for Biological Cybernetics developed a novel approach to motion simulation that provides a larger simulator workspace.

III. MPI CYBERMOTION SIMULATOR

A. Simulator Characteristics

The MPI CyberMotion Simulator, shown in Fig. 2, has several unique features. The basis of the simulator is formed by an anthropomorphic robot arm based on the Robocoaster from KUKA GmbH, Germany, which has similar degrees of freedom to those of a human arm. The robot arm can be equipped with a seat or an actuated cabin, as shown in Fig. 3. The entire assembly is positioned on a linear track with a range of 9.88 m.

All axes of the MPI CyberMotion Simulator are electrically driven, and their characteristics are given in Table 2. The eight degrees of freedom of the simulator are not

Fig. 2. The MPI CyberMotion Simulator (http://www.youtube.com/watch?v=GhnIK1PILig for a video).

Table 2. Characteristics of the MPI CyberMotion Simulator

	Axis	Range	Velocity limit	Acceleration limit
Anthropomorphic robot	1	∞	68°/s	98°/s^2
	2	-128/-48°	57°/s	70°/s^2
	3	-45/+92°	69°/s	128°/s^2
	4	±180°,*	76°/s	33°/s^2
	5	±58°	76°/s	95°/s^2
	6	±180°,*	120°/s	77°/s^2
Actuated cabin	-	1.35 m	0.5 m/s	N/A
Linear track	-	9.88 m	1.5 m/s	N/A

*Limited by cables, otherwise ∞.

124

coupled, and therefore, the motion envelope is extended compared to traditional Stewart platforms. Hence, the simulator can be used to move participants into positions that cannot be attained by a Stewart platform. For example, the enclosed cabin can be positioned above the vertically extended robot arm, such that participants can be rotated along the vertical axis indefinitely, and differential thresholds in yaw can be determined. In a different configuration of the simulator, participants can be positioned in any orientation in the enclosed cabin or the seat, even upside-down, to investigate the influence of gravity on perception.

The performance of the anthropomorphic robot that is part of the CyberMotion Simulator has been evaluated by measuring the transport delay of the system and by determining its frequency response [16].

It was found that the transport delay is equal to 41 ms, and that the system shows mechanical resonance at fre-

quencies depending on the actuator axis. The lowest resonance frequency occurs for the axis at the base of the simulator (axis 1), as it has to drive the largest mass due to the serial configuration of the actuators. Such a configuration can also result in reduced rigidity at the location of the cabin compared to parallel platforms such as a Stewart platform. This results in disadvantages for certain simulator configurations in experimental evaluations where low motion noise is required, such as measurements of motion perception thresholds.

The visualization system of the simulator is different for the seat and the enclosed cabin. In the case of the seat, a curved screen is combined with a single projector and mounted 70 cm in front of the participant as shown in Fig. 3a. The display has an approximate field of view of 90° horizontally 60° vertically. The enclosed cabin has a double-curved projection screen with two projectors (Fig. 3b). The field of view is approximately 140° horizontally and 70° vertically, but the projectors can also be used to display a stereo image with a slightly smaller field of view.
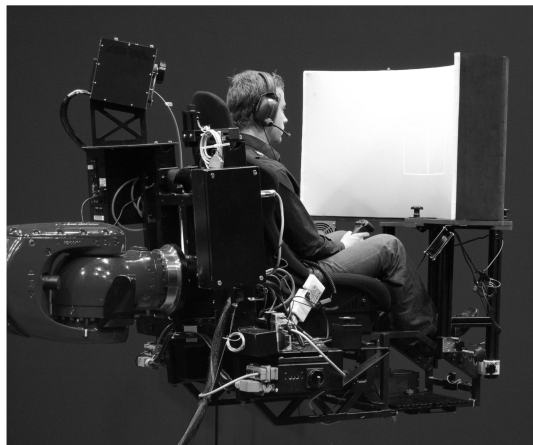
The simulator can be equipped with different input devices, depending on the experimental task. In basic psychophysical experiments, participants typically use button boxes to indicate their response. Furthermore, the enclosed cabin can be equipped with control-loaded devices such as a steering wheel, or a helicopter cyclic stick, collective stick, and pedals.

B. Research Questions

The MPI CyberMotion Simulator is used for various purposes. First of all, the simulator serves as an experimental platform for basic research into motion perception. For example, measurements of thresholds in response to different motion shapes can enhance our understanding of self-motion perception [17]. Also, the large motion range of the simulator allows for performing path integration experiments in three dimensions, such that assessments can be made as to whether path integration is similar between horizontal and vertical planes [18].

The MPI CyberMotion Simulator is also used to investigate the influence of motion in vehicle control tasks such as driving and helicopter flight. This will lead to a better understanding of human behavior in a simulator environment by modeling human control behavior, or to the enhancement of motion simulation by using models of motion perception within the simulator drive algorithms.

In the next section, an experiment is presented that could only be performed on the CyberMotion Simulator, as it features a large motion workspace. The experiment focuses on the influence of rotational and translational motion cues on control behavior in a helicopter hover task (Fig. 4). The CyberMotion Simulator could provide unscaled and unfiltered cues for translational motion, unlike a general Stewart platform. A cybernetic approach was taken in which human behavior was described with

(a)

(b)

Fig. 3. The CyberMotion Simulator with different displays and control interface. The CyberMotion Simulator equipped with a seat and projection system (a) and an enclosed cabin and a stereo projection system (b).
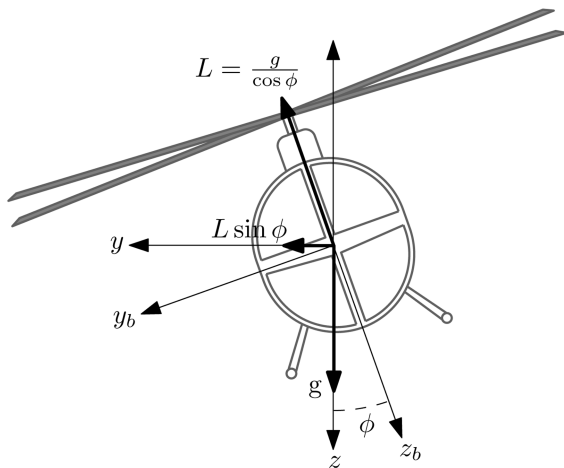
Fig. 4. Forces experienced in a in roll-lateral helicopter maneuver.

Fig. 5. The manual control task.

Fig. 6. A compensatory display, which displays a roll tracking error e_ϕ and a lateral tracking error e_y.

models based on control theory. As such, human behavior can be measured objectively instead of having to rely on subjective metrics.

IV. EXPERIMENTAL HELICOPTER CONTROL TASK

The research in this section is based on the work described in [19].

A. Helicopter Control Task with Roll and Lateral Motion

A helicopter hover task with roll and lateral motion can be modeled as a closed-loop manual control task with a pilot in the loop (Fig. 5). In this control task, the pilot generates a control signal u and actively tracks a target signal f_t, which corresponds to a target helicopter with coordinated roll and lateral motion, while compensating for a disturbance f_d. A compensatory display shows the roll error e_ϕ, which is the difference between the target f_t and the roll angle ϕ (Fig. 6). The roll error e_ϕ results in a coordinated lateral tracking error e_y, which is also presented on the display.

The helicopter flight dynamics are given by the following equations of motion [15]:

$$\ddot{\phi} = -4.5\dot{\phi} + 2.0\delta \qquad (1)$$

$$\ddot{y} = L\sin\phi = g\tan\phi \approx 9.81\phi \qquad (2)$$

In these equations, the translational motion y is fully coordinated with the roll motion ϕ. The parameter δ represents the pilot input, L is the lift vector of the helicopter, and g is the gravity constant of 9.81 m/s^2.

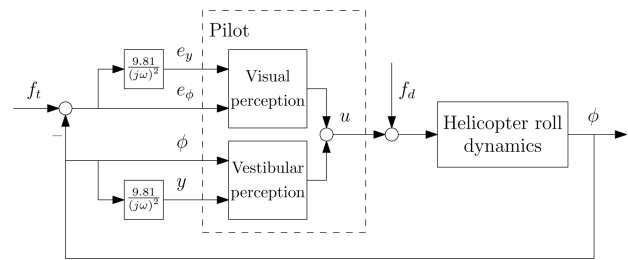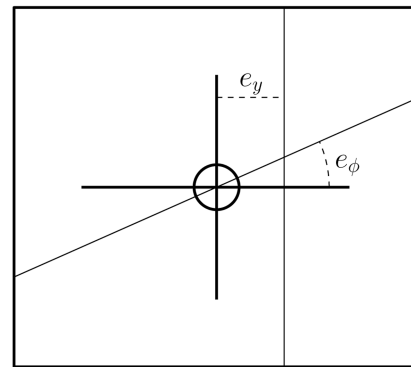### B. Multimodal Pilot Model Identification

In the control task given in Fig. 5, the pilot controls the helicopter dynamics H_h. The visual perception channel is modeled with a visual response function H_{pe}, and the vestibular perception channel is represented by a response to simulator motion $H_{p\phi}$. These pilot response functions can be parameterized with a two-step identification method by determining the input-output relationship and fitting a suitable pilot model [20].

The pilot model considered for this control task is given in Fig. 7, and considers two inputs: e_ϕ and ϕ. The lateral error e_y and lateral position y can be calculated from these inputs with Equation (2). The pilot equalization for both model inputs consists of two parts. The first part relates the lateral cues e_y and y to the pilot control signal u and includes gains $K_{pe,l}$ and $K_{p\phi,l}$, respectively. The second part relates the rotational cues e_ϕ and ϕ to the pilot control signal. Both channels include a gain and a lead time constant: $K_{pe,r}$ and $t_{le,r}$ for channel e_ϕ, and $K_{p\phi,r}$ and $t_{l\phi,r}$ for channel ϕ.

The pilot limitations include the visual time delay τ_e and the motion time delay τ_ϕ. The pilot neuromuscular dynamics H_{nm} are represented by:

$$H_{nm} = \frac{\omega_{nm}^2}{\omega_{nm}^2 + 2\zeta_{nm}\omega_{nm}j\omega + (j\omega)^2} \qquad (3)$$
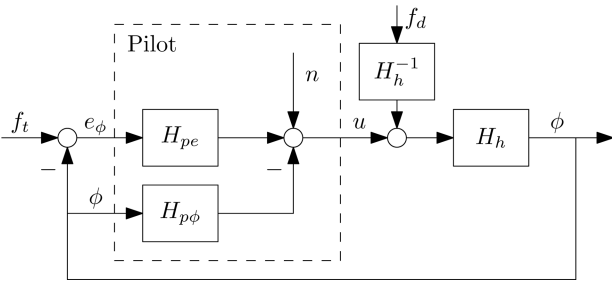
Fig. 7. The multimodal pilot model.

Table 3. Experimental conditions

Condition	Lateral motion	Roll motion
C1	-	-
C2	+	-
C3	-	+
C4	+	+

where ζ_{nm} and ω_{nm} are the neuromuscular damping and frequency, respectively.

The open-loop transfer functions of the control loop can be determined for inputs f_d and f_t, and are given as:

$$H_{ol,d} = (H_{pe} + H_{p\phi})H_h \qquad (4)$$

$$H_{ol,t} = \frac{H_{pe}H_h}{1 + H_{p\phi}H_h} \qquad (5)$$

The crossover frequencies $\omega_{c,d}$ and $\omega_{c,t}$ of $H_{ol,d}$ and $H_{ol,t}$, respectively, indicate performance. The phase margins $\varphi_{m,d}$ and $\varphi_{m,t}$ are a measure for the stability of the control loop.

C. Experiment Setup

To investigate the influence of simulator motion on pilot performance and control behavior, seven participants took part in an experiment in which the roll and lateral motion of the simulator were manipulated independently (Table 3). During the experiment, five repetitions of each condition were presented randomly. Each trial lasted 110 seconds, of which 98.3 seconds were measurement time. The first 11.7 seconds were not used and allowed the participants to stabilize the helicopter dynamics. Data were logged at 12 ms.

The participants performed a target-following disturbance-rejection control task, which was created by inserting a target forcing function f_t and a disturbance forcing function f_d into the closed loop. These forcing functions consisted of multiple sine signals, such that they appeared random to the pilot. These forcing functions were constructed as follows:

$$f_{d,t} = \sum_{k=1}^{N_{d,t}} A_{d,t}(k)\sin(\omega_{d,t}(k)t + \phi(k)) \qquad (6)$$

Where d and t represent the disturbance and target forcing function, respectively. The frequency of the kth sine wave is given by ω, A is the amplitude, and ϕ is the phase. The frequencies were all integer multiples $n_{d,t}$ of the base frequency $\omega_m = 2\pi/T_m = 0.0639$ rad/s. The details of the forcing functions are given in Table 4: and time histories are shown in Fig. 8. The variances of the disturbance and target forcing function were scaled to 1.6 and 0.4 deg^2, respectively, to yield a control task that is predominantly a disturbance-rejection task. The disturbance forcing function was prefiltered with the inverse helicopter dynamics to counteract attenuation when passing through these dynamics.

In this experiment, the MPI CyberMotion Simulator

Table 4. Forcing function data

Disturbance (f_d)				Target (f_t)			
n_d (-)	ω_d (rad/s)	A_d (deg)	ϕ_d (rad)	n_t (-)	ω_t (rad/s)	A_t (deg)	ϕ_t (rad)
5	0.320	1.596	-2.088	6	0.383	0.744	0.537
11	0.703	1.297	1.238	13	0.831	0.567	1.649
23	1.470	0.728	-3.895	27	1.726	0.288	5.033
37	2.365	0.392	3.138	41	2.621	0.161	0.184
51	3.388	0.227	-2.807	53	3.643	0.097	5.836
71	4.666	0.139	-1.808	73	4.858	0.062	4.589
101	6.456	0.087	-1.563	103	6.583	0.040	3.070
137	8.756	0.060	-2.953	139	8.884	0.028	3.635
171	12.208	0.044	-2.626	194	12.400	0.021	1.491
226	17.193	0.035	0.864	229	17.321	0.017	2.883
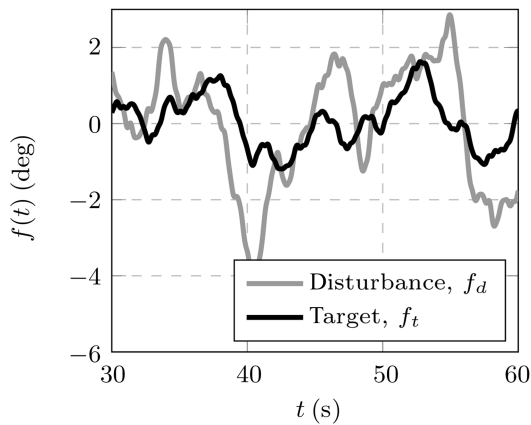
Fig. 8. Time histories of the forcing functions.

Fig. 9. Variance decompositions of the error and control signals for every condition averaged over seven participants. Variance is decomposed into components due to f_t(t), f_d(d), and remnant n(r). (a) Roll error signal, (b) lateral error signal, and (c) control signal.

was used with the seat (Fig. 3a). Roll motion was provided by the axis of the anthropomorphic robot that was closest to the participants, resulting in roll motion around the abdomen. The axis at the base of robot was used to generate lateral motion cues by moving the seat along an arc with a radius of 3.11 m, as the linear track was not yet available. The large motion space of the simulator allowed the experiment to be performed without motion filters. Participants used a cyclic stick with a low stiffness and no breakout force to control the helicopter dynamics. The compensatory display shown in Fig. 6 was projected on the screen in front of the participants. The experiment was conducted in complete darkness to eliminate any visual cues resulting from the static reference frame of the room.

During the experiment, the error signals e_ϕ and e_y, and control signal u were recorded. The pilot response functions H_{pe} and $H_{p\phi}$ were identified from these measured signals, and the parameters of the pilot model were subsequently estimated by fitting the pilot model to the identified response functions [20]. Given the pilot model parameters, the cross-over frequencies and phase margins could be calculated from the open-loop response functions.

D. Results

The tracking performance and control activity of participants were evaluated with the variance of the roll error e_ϕ, the lateral error e_y, and the control signal u (Fig. 9). The contribution of the forcing functions f_d and f_t and the remnant n were considered separately. The roll tracking performance was better when either roll or lateral motion cues were provided to participants, whereas the lateral tracking performance did not depend on the availability of roll motion. Lateral cues had a positive influence on the lateral tracking performance, which indicates their relative importance in this type of control task.

The control activity of participants was not affected by the availability of motion cues. The variance of the control signal clearly shows that the control task was mainly
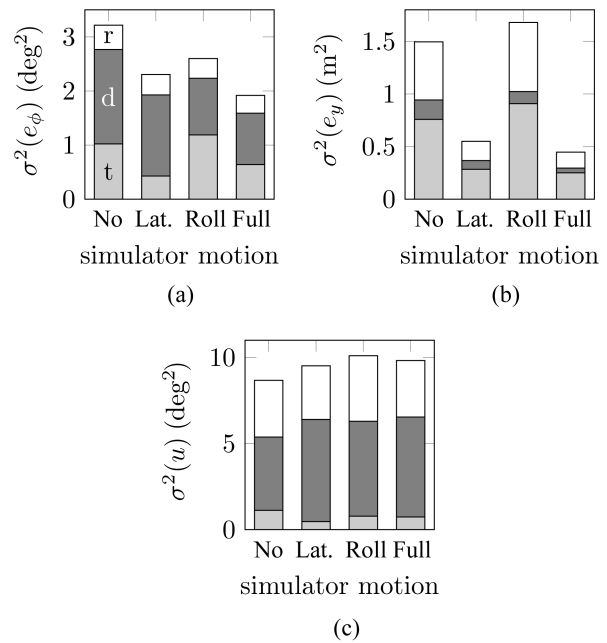
a disturbance-rejection task, as this component constituted the largest part of the measured control signal variance.

Pilot control behavior was assessed by determining the parameters of the pilot model given in Fig. 7 by fitting the model to the visual and vestibular response functions H_{pe} and $H_{p\phi}$. For conditions without simulator motion, the pilot model only consisted of the visual perception path, and parameters for the motion perception channel were not estimated. The results are presented with error bars that represent the interval with 95% confidence that it contains the population mean. These error bars have been corrected for variability between participants by adjusting the participant means for between-participant effects.

The parameters for the visual perception path H_{pe} are given in Fig. 10. The lateral error gain $K_{pe,l}$ was reduced when simulator motion was present, tentatively indicating that participants shift their emphasis from the visual cues to the motion cues. The roll error gain $K_{pe,r}$ was similarly affected in the presence of lateral motion cues, but less with roll motion cues. This could be an indication that lateral cues in the visual display were beneficial for this control task.

The roll error lead constant was only slightly affected by motion cues. When lateral motion was present, the roll error lead constant was increased, indicating that participants generated lead information concerning the roll angle, i.e., information on roll rate. When both roll and lateral motion cues were present, participants generated less lead,
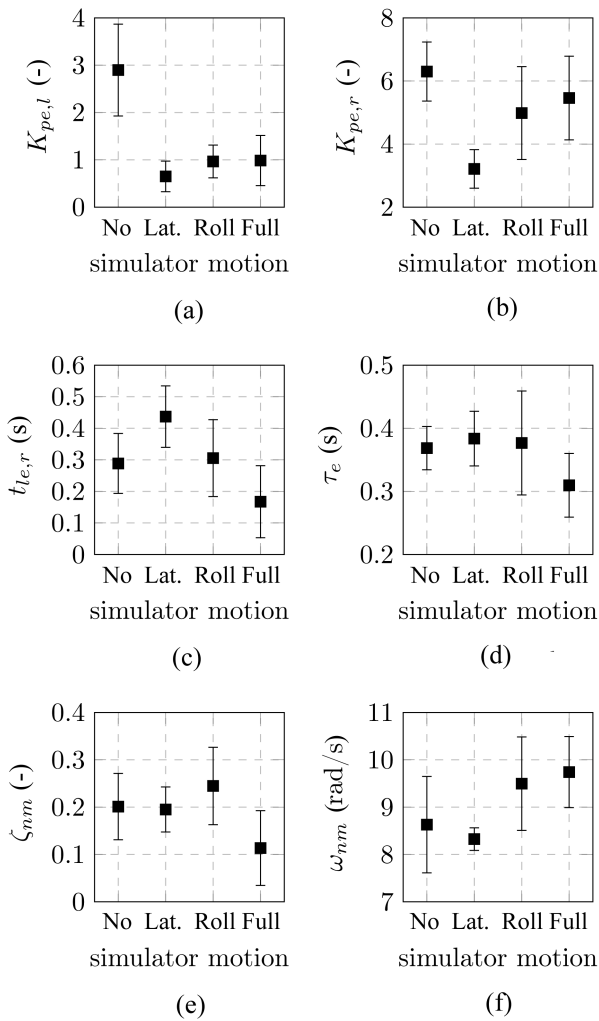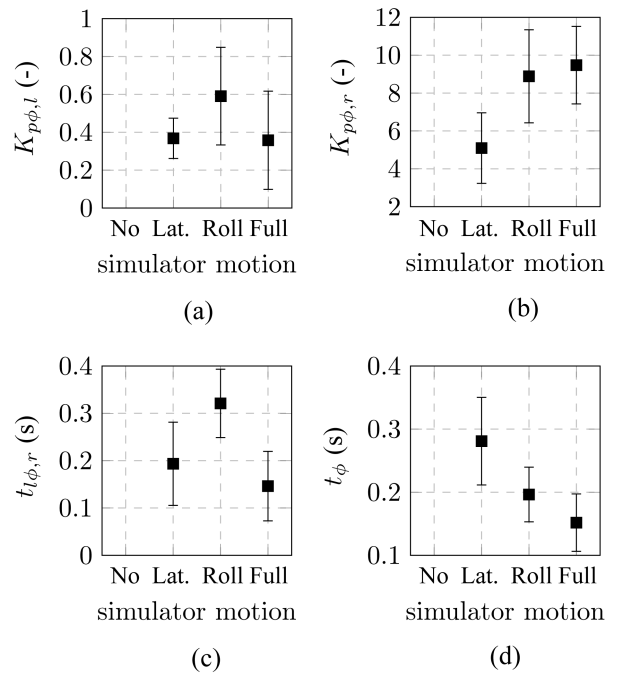
Fig. 10. Pilot model parameters of the visual perception path and the neuromuscular dynamics. (a) Lateral error gain, (b) roll error gain, (c) roll error lead, (d) visual time delay, (e) neuromuscular damping, and (f) neuromuscular frequency.

Fig. 11. Pilot model parameters of the motion perception path. (a) Lateral motion gain, (b) roll motion gain, (c) roll motion lead, and (d) motion time delay.

Fig. 12. Crossover frequencies and phase margins of the open-loop responses. (a) Disturbance crossover frequency, (b) target crossover frequency, (c) disturbance phase margin, and (d) target phase margin.
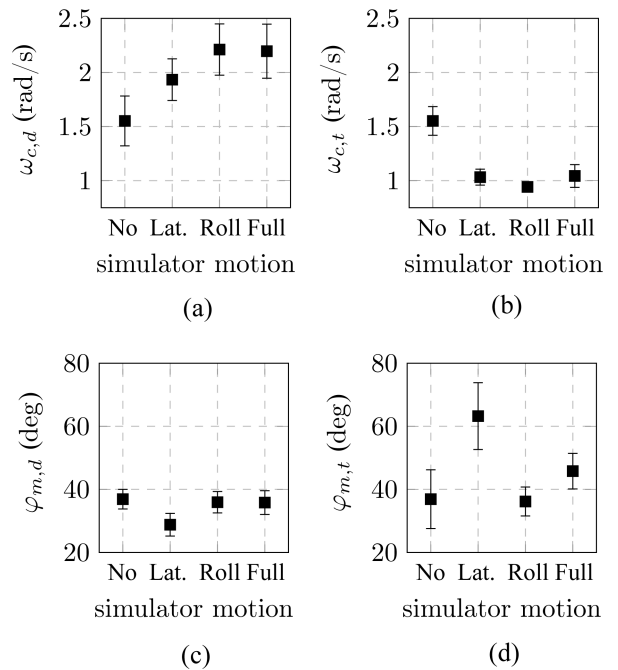
as is indicated by a decrease in the roll error lead constant.

The visual time delay and the neuromuscular damping frequency were not affected by the motion cues. The neuromuscular frequency was slightly increased when roll motion was present, which was indicative of control over an increased bandwidth.

The pilot model parameters for the motion perception path are presented in Fig. 11. Note that these parameters are not defined for the experimental condition without simulator motion. With simulator motion in both degrees of freedom, the motion time delay was decreased further. Tentatively, this indicates the relative importance of simulator motion cues in roll, even though the presence of lateral motion cues provides an additional advantage.

The crossover frequencies and phase margins of the disturbance and target open-loop response functions, presented in Fig. 12, are measures for performance and sta-

bility for attenuation of the disturbance and the target signal. The disturbance crossover frequency increased for

conditions with simulator motion, but was larger when roll motion was available. This is an indication that providing motion cues for the inner roll control loop increased the control bandwidth in this task. The disturbance phase margin was only slightly affected in the presence of only lateral motion, which indicates a decrease in the stability of the control loop.

The target crossover frequency was lower when simulator motion was provided to the participants, which could be the result of participants increasing their performance in the disturbance-rejection task, as indicated by an increase in the disturbance crossover frequency. When lateral motion was provided, the target phase margin was increased, indicating higher stability in the control loop.

V. DISCUSSION

A motion simulator for any type of vehicular control task introduces restrictions on the type of motion cues that can be provided compared to real world motion. The effect of physical motion on human perception and control behavior is not well understood, and studying such effects in a well-defined and controlled manner remains a challenge. The MPI CyberMotion Simulator provides a unique motion platform with a large workspace that can be used to address this challenge. It can produce large linear motion at the pilot station and attain unusual attitudes compared to conventional hexapod motion base simulators.

The MPI CyberMotion Simulator is used to study human perception in low-level psychophysical experiments measuring factors such as motion perception thresholds, and to assess and model performance, perception and control behavior in closed-loop control tasks. Due to the high workspace volume of the simulator, experiments can, in certain conditions, be designed without the motion filters that are typically used to keep the simulator within its motion envelope.

In this paper, an experiment was presented in which the MPI CyberMotion Simulator was used to study multimodal human control behavior using a cybernetic approach. By identifying the visual and vestibular responses of participants in a roll-lateral helicopter hover task, their behavior was described with models based on control theory. Motion feedback to the participants was changed systematically, by providing no motion, only roll motion, only lateral motion, or a combination of roll and lateral motion. The parameters of the identified pilot models provided insight into adaptations of the participants' control strategies due to changes in simulator motion feedback.

Participants were able to increase tracking performance when simulator motion was provided. They changed their control strategy to shift from reliance on visual error perception to reliance on simulator motion cues. Participants showed reduced processing times and control over a higher bandwidth when roll motion was present. The

change in control strategy was also indicated by an increase in the disturbance crossover frequency with both roll and lateral motion, indicating higher performance in reducing the disturbance error.

Future research on the CyberMotion Simulator will focus on technologies that provide assistance to novice pilots, such as haptics and perspective displays. Furthermore, an ongoing project focuses on building models of human perception and developing simulator motion cueing algorithms based on such models.

ACKNOWLEDGMENTS

REFERENCES

1. D. Allerton, *Principles of Flight Simulation*, Chichester, UK: John Wiley and Sons Ltd., 2009.
2. A. T. Lee, *Flight Simulation: Virtual Environments in Aviation*, Aldershot, UK: Ashgate Publishing, 2005.
3. S. K. Advani, "Flight simulation research at the Delft University of Technology to the benefit of aviation safety," in *Aviation Safety: Human Factors, System Engineering, Flight Operations, Economics, Strategies and Management*, Utrecht, the Netherlands: VSP International Science Publishers, 1997, pp. 661-674.
4. R. T. Hays, J. W. Jacobs, C. Prince, and E. Salas, "Flight simulator training effectiveness: a meta-analysis," *Military Psychology*, vol. 4, no. 2, pp. 63-74, 1992.
5. J. Burki-Cohen, N. N. Soja, and T. Longridge, "Simulator platform motion: the need revisited," *International Journal of Aviation Psychology,* vol. 8, no. 3, pp. 293-317, 1998.
6. A. L. Sparko, J. Burki-Cohen, and T. H. Go, "Transfer of training from a full-flight simulator vs. a high level flight training device with a dynamic seat," in *Proceedings of the AIAA Modeling and Simulation Technologies Conference*, Toronto, Canada, 2010, paper no. AIAA-2010-8218.
7. J. C. F. de Winter, D. Dodou, and M. Mulder, "Training effectiveness of whole body flight simulator motion: a comprehensive meta-analysis," *International Journal of Aviation Psychology*, vol. 22, no. 2, pp. 164-183, 2012.
8. R. L. Stapleford, R. A. Peters, and F. R. Alex, "Experiments and a model for pilot dynamics with visual and motion inputs," NASA, Washington, DC, *NASA contractor report no. CR-1325*, 1969.
9. P. M. T. Zaal, D. M. Pool, J. de Bruin, M. Mulder, and M. M. van Paassen, "Use of pitch and heave motion cues in a pitch control task," *Journal of Guidance, Control, and*

Dynamics, vol. 32, no. 2, pp. 366-377, 2009.

10. D. M. Pool, M. Mulder, M. M. van Paassen, and J. C. van der Vaart, "Effects of peripheral visual and physical motion cues in roll-axis tracking tasks," *Journal of Guidance, Control, and Dynamics,* vol. 31, no. 6, pp. 1608-1622, 2008.

11. F. M. Nieuwenhuizen, M. Mulder, M. M. van Paassen, and H. H. Bülthoff, "Influences of simulator motion system characteristics on pilot control behavior," *Journal of Guidance, Control, and Dynamics*, vol. 36, no. 3, pp. 667-676, 2013.

12. D. Stewart, "A platform with six degrees of freedom," *Proceedings of the Institution of Mechanical Engineers,* vol. 180, no. 15, pp. 371-378, 1966.

13. S. K. Advani, "The kinematic design of flight simulator motion-bases," doctoral dissertation, Faculty of Aerospace Engineering, Delft University of Technology, Delft, the Netherlands, 1998.

14. D. Lean and O. H. Gerlach, "Dynamics characteristics of flight simulator motion systems," North Atlantic Treaty Organization, Advisory Group for Aerospace Research and Development, *Tech. Rep. AR-144*, 1979.

15. J. A. Schroeder, "Helicopter flight simulation motion platform requirements," NASA, Washington, DC, *Tech. Rep. NASA/TP-1999-208766*, 1999.

16. H. J. Teufel, H. G. Nusseck, K. A. Beykirch, J. S. Bulter, M. Kerger, and H. H. Bülthoff, "MPI motion simulator: development and analysis of a novel motion simulator," in *Proceedings of the AIAA Modeling and Simulation Technologies Conference and Exhibit*, Hilton Head Island, SC, 2007, paper no. AIAA-2007-6476.

17. F. Soyka, P. Robuffo Giordano, K. Beykirch, and H. H. Bülthoff, "Predicting direction detection thresholds for arbitrary translational acceleration profiles in the horizontal plane," *Experimental Brain Research,* vol. 209, no. 1, pp. 95-107, 2011.

18. M. Barnett-Cowan, T. Meilinger, M. Vidal, H. Teufel, and H. H. Bülthoff, "MPI CyberMotion Simulator: implementation of a novel motion simulator to investigate multisensory path integration in three dimensions," *Journal of Visualized Experiments*, vol. 63, no. 5, pp. 1-6, 2012.

19. F. M. Nieuwenhuizen, P. M. T. Zaal, H. J. Teufel, M. Mulder, and H. H. Bülthoff, "The effect of simulator motion on pilot control behaviour for agile and inert helicopter dynamics," in *Proceedings of the 35th European Rotorcraft Forum,* Hamburg, Germany, 2009.

20. F. M. Nieuwenhuizen, P. M. T. Zaal, M. Mulder, M. M. van Paassen, and J. A. Mulder, "Modeling human multichannel perception and control using linear time-invariant models," *Journal of Guidance, Control, and Dynamics,* vol. 31, no. 4, pp. 999-1013, 2008.
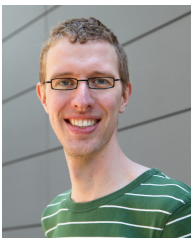
Frank M. Nieuwenhuizen

Frank M. Nieuwenhuizen received his M.Sc. degree in aerospace engineering from Delft University of Technology in 2005 for work on the identification of pilot control behavior in a closed-loop control task and its experimental application. In 2012, he received his Ph.D. degree for his research into the influence of simulator motion system characteristics on pilot control behavior, a collaboration between the Department of Human Perception, Cognition and Action at the Max Planck Institute for Biological Cybernetics and the Faculty of Aerospace Engineering at Delft University of Technology.
He currently works on the myCopter project, which he co-wrote and which is funded by the European Commission under the Seventh Framework Programme.

Heinrich H. Bülthoff

Heinrich H. Bülthoff received his Ph.D. degree in natural sciences and the Ph.D. degree in biology in 1980 from Eberhard Karls University, Tübingen, Germany.
From 1980 to 1988, he was a Research Scientist with the Max Planck Institute (MPI) for Biological Cybernetics, Tübingen, and the Massachusetts Institute of Technology, Cambridge. From 1988 to 1993, he was an Assistant Professor of cognitive science, then an Associate Professor of cognitive science, and finally a Full Professor of cognitive science with Brown University, Providence, RI. In 1993, he became the Director of the Department of Human Perception, Cognition and Action, Max Planck Institute for Biological Cybernetics, and a scientific member of the Max Planck Society. Since 1996, he has been an Honorary Professor with the Eberhard Karls University in Tübingen, Germany, and since 2009 an Adjunct Professor with Korea University, Seoul, Korea.
His research interests include object recognition and categorization, perception and action in virtual environments, and human-robot interaction and perception.